Available online at www.sciencedirect.com
ScienceDirect
Computer Physics Communications 177 (2007) 6–13
Computer Physics Communications
www.elsevier.com/locate/cpc

Materials simulations using VASP—a quantum perspective to materials science

J. Hafner

Faculty of Physics and Center for Computational Materials Science, University of Wien, Sensengasse 8/12, A-1090 Wien, Austria

Available online 23 February 2007

Abstract

The fundamental aspects of ab-initio simulations of materials properties and of processes in materials based on density-functional theory, and their implementation at various levels of theory in the Vienna ab-initio simulation package are reviewed. The state-of-the-art is illustrated at selected examples, chosen from nanostructured materials, quasicrystals, surface science and catalysis. Finally a brief outlook is given on current developments attempting to make post-DFT approaches applicable to materials-science problems.

Keywords: Density functional theory; Materials science; Magnetism; Quasicrystals; Surface science; Catalysis; Intermetallics; Post-DFT approaches

1. Introduction

During the past decade, computer simulations based on a quantum-mechanical description of the interactions between electrons and atomic nuclei have strongly influenced the development of materials science. The impact of quantum mechanics is not restricted to academic research, the current developments are paving the way towards a quantum-based materials design for future technologies.

The task of solving the Schrödinger equation for the complex many-ion, many-electron system of a solid is a very challenging one and accessible only to numerical approaches. The adiabatic approximation allows to decouple the ionic and electronic dynamics since their characteristic time-scales differ by several orders of magnitude. A very important further step was realized when Walter Kohn and co-workers [1] developed density-functional theory which reduces the intractable complexity of the electronic many-body interactions to an effective single-electron equation determined by the exchange–correlation functional which depends on the electron-density only. Although the form of this functional which would make the reformulation of the many-electron Schrödinger equation exact is unknown, approximate functionals have proven highly successful in describing many materials properties. However, even with the simplifications introduced by density-functional theory (DFT) the development of the highly efficient and accurate algorithms required for solving the Kohn–Sham equations for technologically relevant systems is a nontrivial problem. One has to remember that in 1998 Walter Kohn shared the Nobel Prize for Chemistry (which he received for developing the fundamentals of DFT) with John Pople who was rewarded for the development of the GAUSSIAN program package [2] which allows to perform efficient DFT calculations for complex molecular systems. To date GAUSSIAN continues to be the most important tool for performing quantum-chemical calculations on molecules. The equivalent of the GAUSSIAN package for solid-state and materials science still has to be developed. The Vienna ab-initio simulation package VASP developed by Georg Kresse and co-workers [3–7] is only one of many initiatives in that direction [for a recent review see, e.g., the recent issue of the MRS Bulletin dedicated to the impact of DFT on materials science [8]], but probably a very successful one. In the present paper I shall give a concise review of the fundamental principles underlying VASP, followed by a short description of applications in key areas of materials science. The article closes with an outlook on current attempts to account for many-electron correlations beyond DFT and first applications to materials-related problems.

E-mail address: juergen.hafner@univie.ac.at.

0010-4655/$ – see front matter
doi:10.1016/j.cpc.2007.02.045

2. Fundamentals

The most important factors determining the level of theory of a quantum-mechanical computer experiment are the choice of an exchange–correlation functional, the choice of a basis-set for the expansion of the Kohn–Sham orbitals, charge- and spin-densities and potentials, and the algorithm adopted for solving the Kohn–Sham equations and for calculating energies, forces and stresses. The degree to which the chosen functional accounts for many-electron correlations and the completeness of the basis-set determine the accuracy of the calculation, the numerical algorithms are decisive for its efficiency.

2.1. Hierarchy of exchange–correlation functionals

During the last two decades many approximations to the exchange–correlation functional that would produce, within DFT, exactly the same ground-state as the solution of the many-body Schrödinger equation, have been proposed. Perdew [9] refers to the hierarchy of approximate functionals as the "Jacob's ladder" of DFT. The lowest rung on this ladder is the

Local density approximation (LDA). At this level, the local exchange–correlation energy, $E_{\rm xc}[n(\vec{r})]$, is taken to be the same as in a homogeneous electron gas of the same density, as derived from quantum Monte-Carlo simulations.

The *Generalized Gradient Approximation* (GGA) introduces a dependence of $E_{\rm xc}$ on the local gradient of the electron density, $|\nabla n(\vec{r})|$. Many different forms of the GGA have been proposed in the literature. For materials simulations it is good practice to adopt parameter-free functionals derived from known expansion coefficients and sum-rules of many-body theory [10,11] and to avoid empirical parameterizations popular in molecular quantum chemistry.

Meta-GGA functionals introduce the kinetic energy density [or the Laplacian $\Delta n(\vec{r})$ of the electron density] as an additional variable [12].

Hyper-GGA uses the one-electron orbitals (instead of the many-electron wavefunctions) to evaluate the Hartree–Fock exchange energy; this is often referred to as "exact exchange".

Hybrid functionals mix exact (i.e. Hartree–Fock) and DFT exchange and describe correlation at the DFT level [13,14].

All functionals exist in a spin-degenerate and spin-polarized (for magnetic calculations) version. LDA and GGA are by far the most commonly used functionals. The GGA corrects the over-binding tendency of the LDA (albeit with a certain trend to over-correct for heavy elements) and yields a correct answer in some cases where the LDA fails quite spectacularly [such as the prediction of the correct ground-state of Fe (ferromagnetic) and Cr (antiferromagnetic) which are both predicted to be nonmagnetic in the LDA] [15] and the location of the energy barrier for the dissociation of small molecules over metallic surfaces [16]. Climbing the DFT ladder further to the meta-GGA or hyper-GGA does not lead to a systematic improvement over the GGA [17,18]. Hybrid functionals are enormously popular in molecular chemistry, but their application to solid-state and materials problems is still in a pioneering stage. Preliminary studies [19] show a great promise for insulating and semiconducting systems, although serious difficulties are evident if these functionals are applied to metals. Novel range-separated functionals may offer a viable solution also for metals [20]. All levels of DFT have been implemented in VASP, and at the end of this paper I shall comment specifically on the latest results for ground-state properties obtained with hybrid functionals and for the description of excited states based on many-body perturbation theory.

2.2. Basis sets, potentials and pseudopotentials

In practice, the Kohn–Sham equations are solved iteratively, using an expansion of the orbitals in terms of an appropriately chosen set of basis functions. The plane-wave (PW) basis-set adopted in VASP offers two main advantages. (i) Control of basis-set convergence, which is crucial for the accuracy of a calculations (and in particular for the prediction of pressures, forces, and stresses) is almost trivial. Very large local basis sets are required to match the accuracy of a well converged PW calculation [21]. "PW accuracy" has become almost proverbial in the DFT community. (ii) The calculation of the forces acting on the atoms and of the stresses on the unit cell using the Hellmann–Feynman theorem is straightforward. This opens the way to quantum ab-initio molecular dynamics simulations for studying the time-development of a system.

A pre-requisite to the successful use of PW basis sets is to describe the electron–ion interaction by a pseudopotential, eliminating the need for an explicit treatment of the strongly bound and chemically inert core-electrons. The theory of pseudopotentials is mature and modern, so-called "ultrasoft" pseudopotentials have the merit of making calculations for d- and f-electron systems feasible at tractable computational effort [22]. A certain drawback of pseudopotentials is that due to the nonlinearity of the exchange–correlation functional in DFT, elaborate nonlinear core-corrections are required for an accurate description of the valence-core interaction in all systems where the overlap between core- and valence-electron densities is not negligible. The projector-augmented wave (PAW) approach developed by Blöchl [23] and adapted and implemented in VASP by Kresse and Joubert [6] reconstructs the full all-electron density and avoids the necessity of nonlinear core-corrections. The relaxed-core version of VASP-PAW developed recently by Marsman and Kresse [24] definitely puts pseudopotential-based PW calculations at the same level of accuracy as the most accurate all-electron calculations such as the full-potential linearized augmented plane-wave (FLAPW) method (which is, however, computationally much less efficient).

2.3. Solving the Kohn–Sham equations

The most direct approach to the solution of the Kohn–Sham (KS) equations is the straightforward diagonalization of the KS Hamiltonian. For large systems and plane-wave basis sets this is, however, very inefficient, given the size of the Hamiltonian matrix. As a rule of thumb, about 100 to 150 plane waves per atom are required to achieve basis-set convergence. Hence for

systems with a few hundred atoms per cell, the size of the Hamiltonian matrix varies between $10^4 \times 10^4$ and $10^5 \times 10^5$. In addition, not all eigenvalues, but only those of the occupied and of the lowest empty eigenstates are required—and this is usually only 10 percent or even less than the total number of eigenvalues. For this reason, iterative variational approaches are to be preferred over direct diagonalization. The general variational principle of quantum mechanics may be applied either to the total energy, to the KS eigenvalues, or to the norm of the residual vector to an eigenstate. Variational minimization of the total energy may be based on a dynamical-simulated annealing of the coupled electron–ion system [as in the Car–Parrinello (CP) method [25]] or on a conjugate-gradient minimization [26]. Both approaches encounter difficulties when applied to metals—in CP calculations the control of adiabaticity is possible only via Nosé thermostats attached to both the electronic and ionic subsystems, convergence of the minimization of the total electronic energy is hampered by charge fluctuations of the mobile valence electrons. The successful strategy adopted in VASP is based on a band-by-band optimization of the eigenstates via a minimization of the norm of the residual vector to each eigenstate [5]. Minimizing the residual vector instead of the eigenvalue has the advantage that it is free of orthogonality constraints. After updating all required eigenstates, re-orthogonalization by sub-space diagonalization is sufficient and easy. The reduction of the number of orthogonalizations greatly improves the scaling of the computational effort with systems size, scaling remains $O(N^x)$ with $x < 2$ up to very large system size. Together with an optimized pre-conditioned charge- and spin-density mixing, residual minimization is a very stable and efficient strategy for solving the KS equations. For details we refer to the paper by Kresse and Furthmüller [5] and to the VASP homepage [7].

2.4. Tools

Solving the KS equations is not enough—a really useful software-package for materials simulations must offer a set of routines for calculating (and eventually also visualizing) from the eigenstates, energies and forces a wide range of materials properties: atomic, electronic and magnetic structures, spectra (electronic, optical, vibrational, ...), mechanical properties (elastic moduli, theoretical strength, ...), thermodynamic properties (heats of formation, activation energies for phase transformations and chemical reactions, ...), magnetic properties (moments, susceptibilities, anisotropy energies, ...)—this list is far from exhaustive. We refer to the VASP homepage for a more detailed information of the functionalities available in the program package. Recently, the predictive abilities of ab-initio calculations have received a real boost by combining them with genetic algorithms for predicting, e.g., alloy phase stabilities [27], crystal structures [28] or surface structures [29].

2.5. Limitations

DFT calculations for tens of atoms per cell are now extremely fast, calculations for a few hundred atoms are routine if VASP is used in the parallel mode on a cluster of moderate size (10 to 30 processors). The largest systems treated so far using VASP are large supercells with up to 2744 atoms simulating a C-defect in group-III nitrides [30], ab-initio molecular dynamics calculations of solid–liquid coexistence in Al performed by Dario Alfé [31] use up to 1000 Al atoms, and extend over a time-span of about 15 ps.

3. Applications in front-line research

In the following we will illustrate the potential of VASP at the example of applications in key areas of materials science. These examples have been chosen particularly in areas where computer simulations can answer fundamental questions which cannot be addressed by laboratory experiments.

3.1. Unexpected magnetic ordering in nanostructures

It is well known that the magnetic properties of nanostructured materials can differ quite significantly from those of the bulk: Due to the reduced coordination at a surface, in an ultrathin film, in a nanowire or in a cluster, a quite significant enhancement of the magnetic moment can take place, and in some cases nanostructures of usually nonmagnetic materials show spontaneous magnetic ordering. If the epitaxial relationship with the substrate stabilizes a film structure different from that of the bulk material, this can result in a novel type of magnetic ordering. It is very difficult to explore the magnetic structure of nanostructured systems, because information on the local magnetic moments is not available experimentally—evidently in such a case the computer experiment plays a very important role. Very recently, DFT studies have demonstrated the existence of unexpected magnetic ordering in different nanostructured materials with varying dimensions (ultrathin films, nanowires, clusters). All calculations have been performed in a scalar relativistic mode using spin-polarized GGA functional, but if a noncollinear magnetic structure is considered, spin–orbit coupling is included self-consistently. Interesting results include:

(i) The formation of high-moment *ferromagnetic Mn-films* and of *antiferromagnetic Fe-layers* on W(100) substrates, [32,33] induced by the strong hybridization of the d-band of the magnetic overlayer with the d-band of the substrate. Interestingly, Mn films adsorbed on the more dense W(110) surface display $c(2 \times 2)$ in-plane antiferromagnetism (as confirmed by STM studies [34]), and a transition to layered antiferromagnetism for thicker films. The different magnetic ordering in Mn films on (100) and (110) substrates illustrates the important influence of the strain imposed by the epitaxial relation on the magnetic properties of the ad-layer.

(ii) The formation of a *spin-flop phase* in antiferromagnetic tetragonal Mn films on Fe(100) substrates [35], arising from the conflict between the strong ferromagnetic Mn–Fe coupling and the antiferromagnetic interaction in the Mn layer. As shown in Fig. 1, the noncollinear magnetic

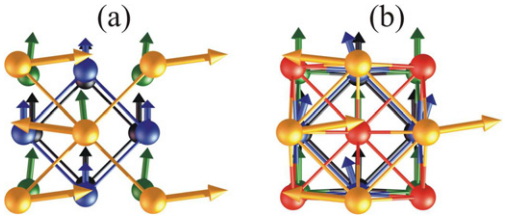

Fig. 1. Noncollinear magnetic structures of the spin-flop phase of Mn mono- (a) and bilayers (b) on a Fe(100) substrate. The arrows show the direction and magnitude of the magnetic moments, Mn-moments in the overlayers are shown in yellow and red (or light gray), Fe-moments in the substrate are given in dark blue and green. After Ref. [35]. (For interpretation of the references to color in this figure legend, the reader is referred to the web version of this article.)

structure with a nearly perpendicular orientation of the Mn-moments relative to the magnetization direction of the substrate releases the strong frustration. For the nearly half-filled Mn d-band, the orbital moment is very small, leading to a very small magnetic anisotropy energy with an easy in-plane orientation.

(iii) Experiments observe a *breakdown of magnetic ordering in Fe–Co nanostructures* on flat and stepped W(110) surfaces with increasing Co-content, but also a strong dependence on preparation conditions. For pseudomorphic submonolayer films, ferromagnetism is found to disappear in the Co-rich regime where antiferromagnetic ordering is preferred. However, for these Co-rich films on W(110) a considerable size-mismatch exists between overlayer and substrate. A full close-packed monolayer can be described by a coincidence lattice of 10 Co atomic rows with 8 underlying W rows along the [001] direction. Two structural models have been proposed, a complete misfit dislocation (where the Co atomic rows are displaced only along the [001] direction), and an incomplete misfit dislocation with simultaneous shifts of Co atoms in both lateral directions (see Fig. 2). An important distinction between these two dislocations is that in the complete misfit dislocation some Co atoms occupy favorable hollow positions and the other unfavorable top positions above the substrate atoms, giving thus rise to a sizeable corrugation, whereas in the incomplete misfit dislocation such extremal positions are avoided. The DFT calculations show that a Co monolayer adopts a structure with the incomplete misfit dislocation network in the ferromagnetic state with a low average magnetic moment of $0.86\mu_B$. The same model is also preferred in the nonmagnetic state, for which very good agreement with STM experiments [37] is achieved. Hence the following consistent picture emerges from the DFT calculations: At lower substrate temperatures the first layer is pseudomorphic to the substrate and forms an antiferromagnetic ground state (but note that because of very small magnetic energy differences the Néel temperature will be very low or magnetic ordering will even be suppressed by fluctuations). In thicker films the second and further layers are close-packed ferromagnetic, but they do not disturb the underlayer. In contrast, at elevated substrate temperatures already the first Co layer will assume a close-packed

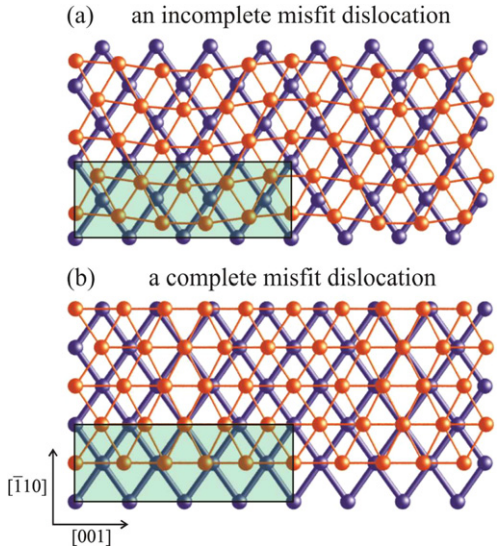

Fig. 2. Structural models for close-packed Co overlayers on W(110): (a) incomplete misfit dislocation and (b) complete misfit dislocation. The (4×1) unit cells containing 8 W and 10 Co atoms are indicated as semitransparent rectangles. After Ref. [36].

structure and hence the whole film is ferromagnetic. In this case the extrapolation of the Curie temperature down to the lowest coverages indicates ferromagnetism.

(iv) DFT calculations also show that Fe–Co monowires on stepped W(970) substrates order antiferromagnetically, because the hybridization with the substrate is particularly strong for a wire at a step-edge [36].

(v) Both ferro- and antiferromagnetic ordering is predicted for monowires of 4d- and 5d-metals supported on vicinal Cu and Ag surfaces, depending on the strain in the monowire imposed by the substrate [38].

(vi) The investigation of the geometric and magnetic structures of small transition-metal (Ni, Pd, Pt, Rh) clusters has revealed the co-existence of structural and magnetic isomers [39]. Surprisingly, already for rather small clusters with 10 to 13 atoms, structures derived from fragments of the crystal structure are found to be more stable than structures based on icosahedral motifs ensuring the closest packing—evidently, this is a consequence of the directional character of d–d bonding. A further interesting aspect of the cluster studies is the importance of the orbital moment: clusters are intermediate between the isolated atom (where the orbital moment is determined by Hund's rule) and the crystal (where the orbital moment of transition metals is almost completely quenched). Fig. 3 shows the results of noncollinear spin-polarized DFT calculations including spin–orbit coupling for a 7-atom Pt-cluster, where all geometric, electronic and magnetic degrees of freedom have been optimized simultaneously. As a consequence of spin–orbit coupling, the magnetic ground state consists of a mixing of different spin-states and canted local spin- and orbitals-moments arising from competing exchange interactions and local magnetic anisotropies. A surprising result is that although the moments on the individual atomic sites are mis-aligned, they add up to

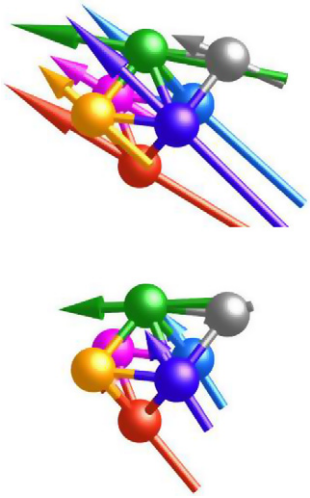

Fig. 3. Noncollinear spin (top) and orbital (bottom) magnetic moments of a Pt_7. Cf. text. After Ref. [40].

collinear total orbital moments and spins of $|\vec{L}| = 1$ and $|\vec{S}| = 2.5$ and a total magnetic moment of $|\vec{M}| = |(\vec{L} + 2 \cdot \vec{S})|\mu_B = 6\mu_B$.

3.2. *Quasicrystals*

The discovery of quasicrystals, i.e. of well ordered solids with long-range noncrystallographic (icosahedral, decagonal) orientational order, but no translation order has been one of the most fascinating developments in modern physics—and at the same time a challenge to both theory and experiment. The challenge to experiment is that without the information on the phase of the scattered radiation, a complete determination of the positions of the atoms in a quasicrystal is impossible (and other techniques such as HRTEM, STM are required to supply at least some additional information). The challenge to theory and simulation is that in the absence of translational periodicity, Bloch's theorem is invalid and in principle calculations have to deal with the infinitely extended crystal. In front of this dilemma, a promising strategy is to perform calculations for a hierarchy of periodic structures (the so-called rational approximants) converging towards the quasiperiodic limit. However, even the lowest order approximant to an icosahedral Al–Pd–Mn quasicrystal has 128 atoms per unit cell, and this number is multiplied by $\tau^3 \sim 4.236..$ (where $\tau = \frac{1+\sqrt{5}}{2}$ is the Golden Mean) at each successive level of the hierarchy—hence calculations on quasicrystalline approximants tend to be quite demanding [41].

Nevertheless, ab-initio DFT calculations have greatly contributed to improve our understanding of the structures and physical properties of quasicrystals. Lately, the attention has focused on the structure and properties of quasicrystalline surfaces and on the formation of quasiperiodically ordered thin films stabilized by the epitaxial relationship with the surface. The particular interest in the surface studies stems from the fact that atomically resolved STM images could in principle give detailed information on the quasicrystalline structure based on the packing of large inter-penetrating icosahedral clusters [42]. For the fivefold surface of icosahedral Al–Pd–Mn, the high-

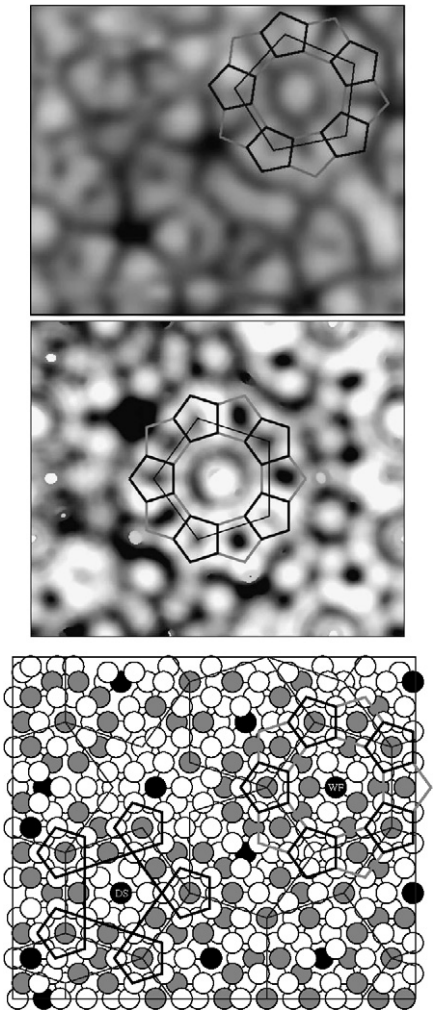

Fig. 4. Experimental (top panel) and calculated (center) STM image of a fivefold surface of icosahedral Al–Pd–Mn, displaying a characteristic feature called the *white star*. The bottom panel shows the underlying atomic structure of the surface as determined by ab-initio structural optimization. White circle—Al, gray—Pd, black—Mn atoms. The characteristic atomic arrangement in a *white flower* and in a *dark star* is indicated. After Ref. [44].

resolution STM experiments have identified two particularly interesting features, nicknamed the "white flower" and the "dark star" [see Fig. 4(a)]. The interpretation of these images, however, turned out to be difficult. Ab-initio calculations based on a surface obtained by cleaving a third-generation approximant (i.e. on a fairly large models already close to the quasiperiodic limit) have not only provided highly accurate information on the stability, geometric and electronic properties of this surface [43], but allow in addition a simulation of the STM contrast [44]. Fig. 4(a) shows a section of the experimental STM image displaying a "white flower", part (b) shows the calculated image, and part (c) the underlying atomic structure of the surface. A white flower and a dark star are highlighted.

A similar analysis has been performed for the tenfold surface of decagonal Al–Ni–Co quasicrystals [45]. On the basis of the successful description of quasicrystalline surfaces, studies of quasiperiodically ordered monolayers have been undertaken. The potential-energy mapping of adatoms on the quasicrys-

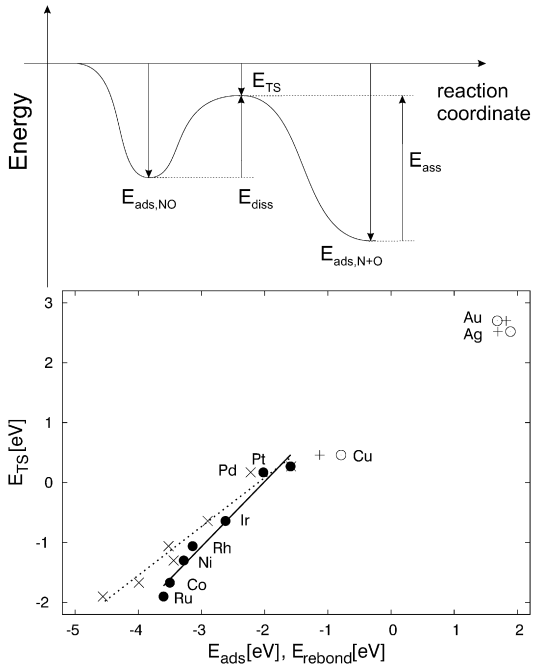

Fig. 5. Potential-energy profile for the dissociation of NO (schematic, top) and the linear BEP relations between the transition-state energies E_{TS} and the dissociative chemisorption (final-state) energies E_{ads} (dots) and the sum of the adsorption energies of isolated N and O atoms, E_{rebond} (crosses)—bottom. After Ref. [52].

talline surface allows to construct detailed models for quasiperiodic single-element monolayers [46] for which experimental studies (based on LEED and Helium-atom scattering) [47] could demonstrate the existence of long-range quasiperiodic order without, however, elucidating the structure on an atomic scale. These studies open the way towards a better understanding of the chemical reactivity of quasicrystalline surfaces.

3.3. Surface science and catalysis

Surface science and catalysis are a field where the progress due to the application of ab-initio DFT-calculation has been particularly impressive—we refer to the recent reviews by Nørskov, Scheffler and Toulhoat on heterogeneous catalysis on metals, oxides and sulfides [48] and by Hafner, Benco and Bucko on acid-based catalysis in mesoporous solids [49]. DFT calculations have not only helped to establish a detailed understanding of some key reactions in heterogenous catalysis [50,51], they have also been invaluable in elucidating trends in chemical reactivities. In particular, DFT calculations of potential-energy profiles of dissociation reactions have shown that the linear free-energy relationships between the transition-state energy E_{TS} for dissociation and the adsorption energy of the dissociated reaction products E_{ads} [known as the Brønsted–Evans–Polanyi (BEP)] relation has a firm theoretical basis. Fig. 5 shows the BEP relation for NO dissociation on the (111) surfaces of transition- and noble-metals [52].

The DFT calculations show that the origin of the linear BEP relation is in the existence of a "late" transition-state and the weak substrate-dependence of the reverse process, i.e. the associative formation of NO molecules from co-adsorbed N and O atoms. Similar BEP relations have been established for a number of dissociation reactions [48], and BEP relations are a core ingredient in rationalizing a vast amount of experimental data.

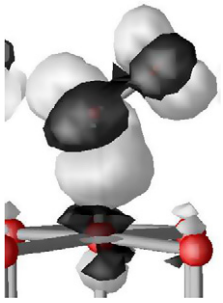

Fig. 6. Charge flow diagram (difference electron densities) for the stable tilted adsorption geometry of NO on NiO(100), taken from spin-polarized GGA+U calculations. Dark color represents depletion, bright color accumulation of electrons. After Ref. [53]. (For interpretation of the references to color in this figure legend, the reader is referred to the web version of this article.)

DFT calculations have also contributed to the development of a really predictive surface- and thin-film-crystallography. This is an important achievement since in many cases the structure of, e.g., surface oxides differs significantly from that of the bulk. A very illustrative example in this field is the combined investigation, using STM experiments and VASP calculations, of the growth of thin oxide layers on the low-index surfaces of Rh [55–57] and of Al_2O_3 films grown on a NiAl(110) substrate [58]. In any case, a determination of the surface structure was possible only via the ab-initio relaxation of models of varying stoichiometry and geometry, and the confrontation of the simulated and measured STM contrast images.

4. Summary and outlook: Towards post-DFT calculations

Ab-initio DFT calculations of materials properties and simulations of processes in materials using VASP are evidently based on a mature methodology, but the quest for higher accuracy and better predictive abilities continues. The work of Georg Kresse and his co-workers has added important post-DFT functionalities to VASP.

DFT calculations for strongly correlated systems such as transition-metal oxides suffer from the incorrect treatment of self-interactions within DFT—evidently for such systems a description at a higher level is theory is required. The simplest correction is based on the so-called DFT+U approach. Here a Hubbard-type on-site Coulomb repulsion between the electrons occupying narrow, strongly correlated bands is added to the KS Hamiltonian. Calculations for NiO, Fe_2O_3 (hematite) and Cr_2O_3 (chromia) show that this results in an improved description of band-gaps, magnetic moments, and bulk and surface structure. A nice example is the investigation of the adsorption of CO and NO on NiO surfaces. The DFT+U approach [53] predicts correctly both the adsorption energy and the unusual tilted adsorption geometry (see Fig. 6—note that the tilted geometry allows for an interaction between the π-orbitals of the molecule and the d_{z^2} of Ni, which is symmetry-forbidden in an upright geometry), whereas both DFT and quantum-

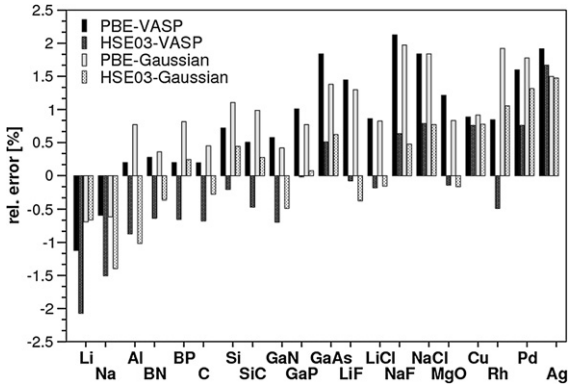

Fig. 7. Lattice constants of solids, calculated using conventional (PBE [11]) and hybrid (HSE03 [14]) functionals, and comparing results obtained with GAUSSIAN and VASP. After Ref. [19].

chemical approaches fail. The earlier results had even inspired experimentalists to announce the "failure of current theoretical methods" for the description of molecular bonding on oxide surfaces [54]. However, a detailed analysis of the band dispersion in comparison with angular-resolved photoelectron spectroscopy show that—although an efficient and accurate tool for calculating materials properties—this is not the definitive answer for the electronic spectrum.

The implementation of hybrid functionals in VASP has been thoroughly tested for molecules against calculations based on GAUSSIAN, with very good success and highlighting the advantages of easy control of basis-set convergence in PW calculations [21]. Tests of hybrid functionals including full and screened Fock-exchange for solids [19] demonstrate a significant improvement in the predicted lattice constants and bulk moduli for semiconductors and insulators over the results obtained with conventional GGA functionals (see Fig. 7), but not for metallic systems. In metallic systems, the exchange-splitting is significantly overestimated, leading to a poor description of itinerant magnets. On the other hand, the plane-wave implementation of screened range-separated hybrid functionals [14] in VASP is efficient enough to allow a treatment of quite complex materials such as strongly correlated transition-metal oxides or zeolites with small and medium-size unit cells. First calculations for insulating antiferromagnetic MnO [59] based on hybrid functionals show that the results for band-gaps and exchange splitting match the DFT+U results, and bring in addition an improved description of the band-dispersion.

However, it should not be forgotten that DFT is based on a theorem relating to the many-electron ground state only. Correct predictions on band-gaps should be based on a correct quasi-particle picture. The GW method [60,61] is a frequently used many-body perturbation expansion for an improved prediction of energy-gaps, band widths, and excited-state energies. GW calculations have been performed at various levels of sophistication, using different approximate forms of the Greens function G and of the screened potential W and different wavefunctions. The calculations published in the literature cover the entire range from non-self-consistent calculations using model Greens functions and potentials (this is commonly called G_0W_0) to self-consistent calculations of both G and W, using quasiparticle wavefunctions—with a strong increase of the computational effort with increasing degree of sophistication. The problem is that the improvement over the G_0W_0 approach is not systematic and trends are obscured by the multiplicity of approximations. Very recently, Shishkin and Kresse [62] have implemented the GW approach in VASP and performed a systematic comparative study for a wide range of insulators and semiconductors, ranging from narrow-gap (PbSe, PbTe) to wide-gap (MgO, LiF, Ar) materials. The result is that at the highest level of theory (self-consistent Greens function and dielectric matrix, quasiparticle wavefunction), the DFT error (too small gaps) is over-corrected. It has already been argued that this might be due to the neglect of vertex corrections in W, which provide an additional screening of the attractive electron–hole interaction [62,63]. Vertex-corrected self-consistent GW calculations and the development of a GW code efficient enough to allow calculations on complex systems such a defects in semiconductors or band-offsets at interfaces are a timely challenge to theory.

In this paper I have attempted to present a glimpse on the state-of-the-art of ab-initio calculations in materials science performed using VASP. The efficiency of the DFT calculations allows to attack complex problems and opens access to many different areas of materials research. At the present moment the great challenge is to improve the predictive ability of the DFT functionals and to add post-DFT functionalities.

Acknowledgements

Stimulating discussion with Georg Kresse are gratefully acknowledged, as well as communication of unpublished material. I also thank Marian Krajci and Daniel Spisak for discussions and long-term cooperation.

References

[1] P. Hohenberg, W. Kohn, Phys. Rev. B 136 (1964) 864;
W. Kohn, L.J. Sham, Phys. Rev. A 140 (1964) 1133.
[2] W.J. Hehre, R.F. Stewart, J.A. Pople, J. Chem. Phys. 51 (1969) 2657; this is the first of a long series of articles describing the theoretical foundations of the GAUSSIAN program package.
[3] G. Kresse, J. Hafner, Phys. Rev. B 48 (1993) 13115.
[4] G. Kresse, J. Hafner, Phys. Rev. B 49 (1994) 14251.
[5] G. Kresse, J. Furthmüller, Comp. Mater. Sci. 6 (1996) 15; Phys. Rev. B 54 (1996) 11169.
[6] G. Kresse, D. Joubert, Phys. Rev. B 59 (1999) 1758.
[7] VASP code, http://cms.mpi.univie.ac.at/vasp/.
[8] J. Hafner, C. Wolverton, G. Ceder, MRS Bulletin 31 (2006) 659.
[9] J.P. Perdew, K. Schmidt, in: V. van Doren, et al. (Eds.), Density Functional Theory and its Application to Materials, American Institute of Physics, Melville, NY, 2001, p. 1.
[10] J.P. Perdew, et al., Phys. Rev. B 46 (1992) 6671.
[11] J.P. Perdew, K. Burke, M. Ernzerhof, Phys. Rev. Lett. 77 (1996) 3865.
[12] J. Tao, et al., Phys. Rev. Lett. 91 (2003) 146401.
[13] J.P. Perdew, M. Ernzernhof, K. Burke, J. Chem. Phys. 105 (1996) 9982.
[14] J. Heyd, G.E. Scuseria, M. Ernzerhof, J. Chem. Phys. 118 (2003) 8207.
[15] E.G. Moroni, et al., Phys. Rev. B 56 (1997) 15629.
[16] A. Gross, Surf. Sci. Rep. 32 (1998) 291.
[17] V.N. Staroverov, et al., Phys. Rev. B 69 (2004) 075102.
[18] F. Mittendorfer, J. Hafner, J. Phys. Chem. B 106 (2002) 13299.

[19] J. Paier, et al., J. Chem. Phys. 124 (2006) 154709.
[20] I.C. Gerber, J.G. Ángyán, Chem. Phys. Lett. 415 (2005) 100.
[21] J. Paier, et al., J. Chem. Phys. 122 (2005) 234102.
[22] D. Vanderbilt, Phys. Rev. B 41 (1990) 7892;
G. Kresse, J. Hafner, J. Phys.: Condens. Matter 6 (1994) 8245.
[23] P.E. Blöchl, Phys. Rev. B 50 (1994) 17953.
[24] M. Marsman, G. Kresse, J. Chem. Phys. 125 (2007) 104101.
[25] R. Car, M. Parrinello, Phys. Rev. Lett. 55 (1985) 2471.
[26] T.A. Arias, M.C. Payne, J.D. Joannopoulos, Phys. Rev. B 45 (1992) 1538.
[27] G.H. Johannesson, et al., Phys. Rev. Lett. 88 (2002) 255506.
[28] D.M. Deaven, K.M. Ho, Phys. Rev. Lett. 75 (1995) 288;
A.R. Oganov, C.W. Glass, S. Ono, Earth Planet. Sci. Lett. 241 (2006) 95.
[29] L. Köhler, Thesis, Universität Wien 2007, unpublished.
[30] L.E. Ramos, et al., Phys. Rev. B 66 (2002) 075209.
[31] D. Alfé, Phys. Rev. B 68 (2003) 064423.
[32] D. Spisak, J. Hafner, Phys. Rev. B 70 (2004) 195426.
[33] S. Dennler, J. Hafner, Phys. Rev. B 72 (2005) 214413.
[34] S. Heinze, et al., Science 288 (2000) 1805.
[35] J. Hafner, D. Spisak, Phys. Rev. B 72 (2005) 144420;
C. Grazioli, et al., Phys. Rev. Lett. 95 (2005) 117201.
[36] D. Spisak, J. Hafner, Phys. Rev. B 70 (2004) 014430.
[37] M. Pratzer, H.J. Elmers, M. Getzlaff, Phys. Rev. B 67 (2003) 153405.
[38] D. Spisak, J. Hafner, Phys. Rev. B 67 (2003) 214416.
[39] T. Futschek, M. Marsman, J. Hafner, J. Phys.: Condens. Matter 17 (2005) 5927; J. Phys.: Condens. Matter 18 (2006) 9703.
[40] T. Futschek, et al., in preparation.
[41] J. Hafner, M. Krajci, in: Z.M. Stadnik (Ed.), Physical Properties of Quasicrystals, Springer, Berlin–Heidelberg, 1999, p. 209.
[42] J. Ledieu, et al., Surf. Sci. Lett. 492 (2001) 729.
[43] M. Krajci, J. Hafner, Phys. Rev. B 71 (2005) 054202.
[44] M. Krajci, et al., Phys. Rev. B 73 (2006) 024202.
[45] M. Krajci, J. Hafner, Phys. Rev. B 73 (2006) 134203.
[46] M. Krajci, J. Hafner, Phys. Rev. B 71 (2005) 184207.
[47] K.J. Franke, et al., Phys. Rev. Lett. 89 (2002) 156104.
[48] J.K. Nørskov, M. Scheffler, H. Toulhoat, MRS Bull. 31 (2006) 669.
[49] J. Hafner, L. Benco, T. Bucko, Topics in Catalysis 37 (2006) 41.
[50] K. Reuter, D. Frenkel, M. Scheffler, Phys. Rev. B 73 (2006) 045433.
[51] K. Honkala, et al., Science 307 (2005) 505.
[52] M. Gajdos, J. Hafner, A. Eichler, J. Phys.: Condens. Matter 18 (2006) 41.
[53] A. Rohrbach, J. Hafner, G. Kresse, Phys. Rev. B 69 (2004) 075413; Phys. Rev. B 71 (2005) 045405.
[54] J.T. Hoeft, et al., Phys. Rev. Lett. 87 (2001) 086101.
[55] L. Köhler, et al., Phys. Rev. Lett. 93 (2004) 266103.
[56] J. Gustafson, et al., Phys. Rev. B 71 (2005) 115442.
[57] C. Dri, et al., J. Chem. Phys. 125 (2006) 094701.
[58] G. Kresse, et al., Science 308 (2005) 1440.
[59] C. Franchini, et al., Phys. Rev. B 72 (2005) 045132.
[60] L. Hedin, Phys. Rev. A 139 (1965) 796.
[61] F. Aryasetiawan, O. Gunnarson, Rep. Prog. Phys. 61 (1998) 237.
[62] M. Shishkin, G. Kresse, Phys. Rev. B 74 (2006) 226402.
[63] M. van Schilfgaarde, T. Kotani, S. Faleev, Phys. Rev. Lett. 96 (2006) 226402.